Journal of Biotechnology 280 (2018) 11–18

Contents lists available at ScienceDirect

Journal of Biotechnology

journal homepage: www.elsevier.com/locate/jbiotec

Comprehensive analysis of a metabolic model for lipid production in *Rhodosporidium toruloides*

María Teresita Castañeda[a,b,1,*], Sebastián Nuñez[b,1], Fabricio Garelli[b], Claudio Voget[a], Hernán De Battista[b]

[a] Centro de Investigación y Desarrollo en Fermentaciones Industriales (CINDEFI), UNLP-CONICET, Facultad de Ciencias Exactas, Universidad Nacional de La Plata, Argentina
[b] Grupo de Control Aplicado (GCA), Instituto LEICI, UNLP-CONICET, Facultad de Ingeniería, Universidad Nacional de La Plata, Argentina

ARTICLE INFO

Keywords:
Metabolic modeling
Lipid production
Rhodosporidium toruloides
Flux balance analysis

ABSTRACT

The yeast *Rhodosporidium toruloides* has been extensively studied for its application in biolipid production. The knowledge of its metabolism capabilities and the application of constraint-based flux analysis methodology provide useful information for process prediction and optimization. The accuracy of the resulting predictions is highly dependent on metabolic models. A metabolic reconstruction for *R. toruloides* metabolism has been recently published. On the basis of this model, we developed a curated version that unblocks the central nitrogen metabolism and, in addition, completes charge and mass balances in some reactions neglected in the former model. Then, a comprehensive analysis of network capability was performed with the curated model and compared with the published metabolic reconstruction. The flux distribution obtained by lipid optimization with flux balance analysis was able to replicate the internal biochemical changes that lead to lipogenesis in oleaginous microorganisms. These results motivate the development of a genome-scale model for complete elucidation of *R. toruloides* metabolism.

1. Introduction

In the last decades, microbial lipids have garnered much attention as an alternative to plant oil, because they are independent of food supply and easy to produce (Karamerou et al., 2017). These biolipids are extensively studied for their application in the production of biofuels and high-value nutritional oils (Béligon et al., 2016; Rutter et al., 2015; Yang et al., 2014; Koutinas et al., 2014; Xu et al., 2013; Xue et al., 2013; Papanikolaou and Aggelis, 2011b). Microbial lipids or single-cell oils (SCO) are produced by several oleaginous microorganisms (bacterium, yeast, algae and filamentous fungus) capable of accumulating more than 20% of their dry weight in lipids, mainly as neutral lipids in triglyceride (TAG) form. In oleaginous microorganisms, *de novo* lipogenesis is a secondary anabolic activity, since lipid accumulation takes place when carbon is in excess and a key nutrient, such as nitrogen, is scarce (Papanikolaou and Aggelis, 2011a). Under these conditions, cellular growth is limited, and the excess of carbon is channeled into lipid bodies (Ageitos et al., 2011).

Oily yeasts have some advantages compared with other oleaginous microorganisms, like short duplication times, nutritional versatility and ease to scale-up for industrial application (Ageitos et al., 2011). Even though *Yarrowia lipolytica* is the best-characterized oleaginous yeast, *Rhodosporidium toruloides* has an enormous potential for SCO production considering that it natively produces lipids at high titers during growth on glucose and has more nutritional versatility than the wild-type *Y. lipolytica* (Zhang et al., 2014). The lipid productivity of *R. toruloides* varies according to the strain, the quality of the culture medium and the culture conditions, as summarized in Table 1. The complete elucidation of lipogenic metabolism of *R. toruloides* is crucial for the development of efficient cultivation processes capable of yielding the lipid productivity needed for its industrial application.

Metabolism can be studied using metabolic models, which contain all relevant metabolic reactions. Furthermore, the application of constraint-based metabolic modeling (CBM) and *in silico* analysis is useful to elucidate the physiological behavior and metabolic states of an organism upon various environmental/genetic changes. Flux balance analysis (FBA) is a methodology capable of predicting the phenotype (flux distribution) that is expressed under certain culture conditions. These predictions are obtained by the optimization of an objective function which represents the optimal behavior of the microorganism,

* Corresponding author.
E-mail address: castaneda@biotec.quimica.unlp.edu.ar (M.T. Castañeda).
[1] These authors are equal contributors.

https://doi.org/10.1016/j.jbiotec.2018.05.010
Received 18 December 2017; Received in revised form 27 April 2018; Accepted 16 May 2018
Available online 19 May 2018
0168-1656/

Table 1
Recent reports of lipid production using *R. toruloides*.

Strain	Lipid (%)	Limitation	Carbon source	Culture	Reference
AS 2.1389	69.5	N	Crude glycerol	B	Xu et al. (2012)
AS 2.1389	47.0	N	Distillery wastewater	B	Ling et al. (2013)
AS 2.1389	61.8	N	Glucose	C	Shen et al. (2013)
AS 2.1389	37.9	N and P	Myristic acid	B	Yang et al. (2015)
AS 2.1389	63.5	N and P	Oleic acid	B	Yang et al. (2015)
DSMZ 4444	58.7	N	Lignocellulosic hydrolysate	B	Fei et al. (2016)
DSMZ 4444	61.5	N	Lignocellulosic hydrolysate	FB	Fei et al. (2016)
NCYC 921	17.27	N	Carob pulp syrup	B	Freitas et al. (2014)
Y4	62.1	P	Glucose	B	Wu et al. (2010)
Y4	43.3	N	Jerusalem artichoke	B	Zhao et al. (2010)
Y4	56.5	N	Jerusalem artichoke	FB	Zhao et al. (2010)
Y4	60.4	N	Glucose	FB	Zhao et al. (2011)
Y4	56.8	S	Glucose	B	Wu et al. (2011)

Cultivation mode: batch (B), fed-batch (FB), continuous (C).

subjected to a number of constraints (Varma and Palsson, 1994; Edwards et al., 2002; Kauffman et al., 2003; Llaneras and Picó, 2008; Orth et al., 2010) (also see references therein).

Few metabolic models have been proposed to describe lipid production in oleaginous microorganisms (Mishra et al., 2016; Kavšček et al., 2015; Ye et al., 2015; Loira et al., 2012; Pan and Hua, 2012). To the best of our knowledge, the first metabolic model for lipid production by *R. toruloides* was reported in Bommareddy et al. (2015). This model represents a significant step towards a better understanding of *R. toruloides* metabolism. Consequently, it should guide further improvements aiming at predicting the *de novo* lipid accumulation and cell mass production under different scenarios. In this work, we present a small-scale metabolic model obtained from curation of the original reconstruction proposed by Bommareddy et al. (2015). By means of FBA, a comprehensive analysis of the network capability was performed for model quality assessment and validation.

2. Materials and methods

2.1. Published metabolic model for R. toruloides

As mentioned above, an earlier metabolic model (referred here as original model) for *R. toruloides* was constructed by Bommareddy et al. (2015), considering the current knowledge from literature (Kumar et al., 2012; Zhu et al., 2012; Liu et al., 2009) and the protein database UniProtKB (Magrane and UniProt Consortium, 2011). This model includes 85 reactions, 69 metabolites and 2 compartments (cytosol and mitochondria) and comprises the main metabolic pathways: glycolysis, pentose phosphate (PP) pathway, tricarboxylic Acid (TCA) cycle and glyoxylate cycle. The model also considers the uptake reactions of four carbon sources (glucose, glycerol, xylose and arabinose), NH_3, O_2, SO_4^{2-}, and the efflux reactions for CO_2, TAG, Cell mass and ATP (to consider maintenance).

In the original model, TAG is synthesized from three molecules of C_{16}PAL (fatty acid used as reference) and glycerol 3-phosphate (glyc3p) (Eq. (1)). For the fatty acids (FAs) synthesis, cytosolic Acetyl-CoA (AcCoA) is needed as well as energy (ATP) and reducing power (NADPH) (Eq. (2)). In addition, glyc3p is obtained from dihydroxyacetone phosphate by Glycerol-3-phosphate dehydrogenase (GDP1) or Glycerol kinase (GUT1) when glycerol is added to the culture medium.

$$GLYC3P + 3C_{16}PAL \rightarrow TAG \quad (1)$$

$$8AcCoA + 7ATP + 14NADPH \rightarrow C_{16}PAL + 7ADP + 14NADP \quad (2)$$

2.2. Complete curation of the original metabolic model

Despite the quality of a metabolic model, it is common for metabolic reconstructions to contain some imbalanced stoichiometries, incomplete pathways, and metabolic gaps. To improve the reconstruction, manual curation must be performed by using data from many different databases.

In this section, the curation of the original reconstruction is described. First, the reactions involved in nitrogen metabolism were unblocked in order to consider nitrogen uptake during growth (Section 2.2.1). Then, a set of reactions was modified to obtain mass and charge balanced equations by adding phosphate (Pi), protons (H^+), water (H_2O) and Coenzyme-A (CoA) (Section 2.2.2). Finally, membrane transporters were revised and the complete compartmentalization of the model was obtained by separating ATP, ADP, and CoA between cytosolic and mitochondrial compartments (Section 2.2.3).

2.2.1. Central nitrogen metabolism in R. toruloides

The nitrogen source incorporated from the culture medium to support cell growth leads to three key compounds: ammonium (NH_4^+), glutamate (glut) and glutamine (glum). In the metabolism of *R. toruloides* these metabolites are linked by the anabolic reactions NADPH-dependent glutamate dehydrogenase (GDH1) that produces glutamate from α-ketoglutarate and ammonia, and glutamine synthetase (GLN1) that synthesizes glutamine by ammonia and glutamate. There are also two catabolic reactions: the NADH-dependent glutamate synthase (GLT1) used to produce glutamate when glutamine is the sole nitrogen source, and NAD+-linked glutamate dehydrogenase (GDH2) that releases ammonia from glutamate (Zhu et al., 2012).

In the original model, the central nitrogen metabolism is represented by the following reactions:

$$NH3t: \rightarrow NH3[c] \quad (3)$$

$$GLN1: ATP + NH3[c] + GLUT[c] \rightarrow GLUM[c] + ADP \quad (4)$$

$$GLT1: AKG[c] + GLUM[c] + NADH[c] \rightarrow 2\,GLUT[c] + NAD[c] \quad (5)$$

where Eq. (3) is the NH_3 uptake reaction and [c] denotes the cytosolic compartment.

From the former reactions it results that there is no reaction in the original model that consumes nitrogen precursors. Therefore, no nitrogen uptake is possible at steady state and, consequently, the reaction of ammonia uptake is blocked. Moreover, the cell mass reaction in the original reconstruction does not take into account glutamine, glutamate or other precursors with nitrogen. The importance of glutamate and glutamine as cell mass precursors, and consequently the central nitrogen metabolism, becomes apparent by highlighting their involvement in transamination reactions required for the synthesis of L-amino acids, and the biosynthesis of purines and pyrimidines (Ljungdahl and Daignan-Fornier, 2012).

To overcome both problems (blocked reactions and the absence of nitrogen compounds as cell mass precursors), we incorporated glutamine and glutamate in the pseudoreaction that represents cell mass

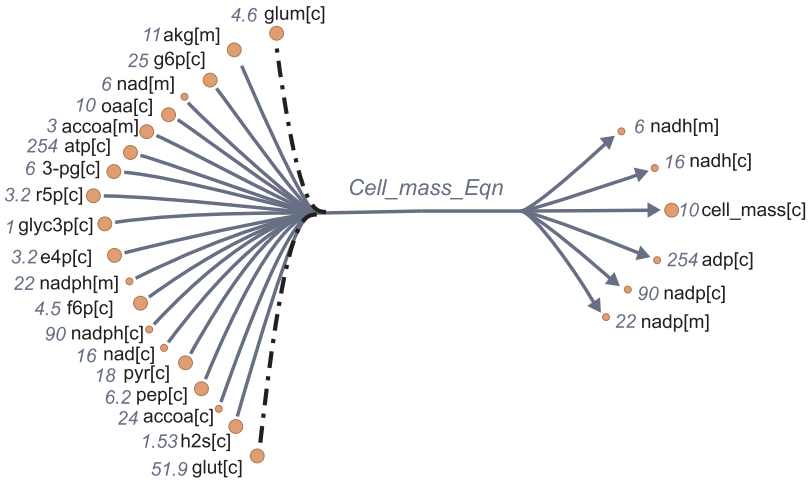

Fig. 1. Incorporation of glutamine and glutamate metabolites in the original cell mass reaction (dashed line).

formation (Fig. 1) and added glutamate dehydrogenase reactions (Eqs. (6) and (7)). Due to the absence of a published empirical cell mass reaction for *R. toruloides*, the glutamate and glutamine coefficients were stoichiometrically calculated by considering an average elemental formula of $CH_{1.76}O_{0.58}N_{0.16}$ (Zhou et al., 2012; Koutinas et al., 2014; Shen et al., 2017). Then, 85% of the total nitrogen required for cell mass production was incorporated as glutamate and 15% was derived from glutamine (Ljungdahl and Daignan-Fornier, 2012).

$$\text{GDH1: AKG[c] + 2H[c] + NADPH[c] + NH3[c] → GLUT[c] + H2O[c] + NADP[c]} \quad (6)$$

$$\text{GDH2: GLUT[c] + H2O[c] + NAD[c] → AKG[c] + 2H[c] + NADH[c] + NH3[c]} \quad (7)$$

2.2.2. Mass and charge balance of the reactions involved in the metabolism

An essential stage in model curation is to detect mass and charge imbalanced reactions in the metabolic network. By using computational methods we found a number of mass imbalanced reactions in the original model (Supplementary data Section S1.2.1). In most cases, the imbalance arises from the omission of a cofactor and other metabolites. With the aim of obtaining a more accurate model for process simulation under different conditions, we modified these reactions by incorporating Pi, H^+, H_2O and CoA when necessary. Besides mass, the model was also balanced in charge considering that all compartments have a physiological pH of 7.2 (Orij et al., 2009). The addition of ionized compounds, protons, and water to charge imbalanced reactions was sufficient to ensure that almost all reactions had no net charge. The only mass and charge imbalanced reaction in the model is the pseudo-reaction of cell mass production. To maintain intracellular physiological pH, a net production (or consumption) of protons had to be balanced by membrane transporters between compartments and with the extracellular medium (for more details see Section 2.2.3).

To perform mass and charge balances, we checked each reaction in the available literature and databases including BiGG Models knowledgebase (King et al., 2016), UniProtKB (Magrane and UniProt Consortium, 2011) and *Saccharomyces* Genome Database (SGD) (Cherry et al., 2012). Since the *R. toruloides* metabolism has not been completely elucidated, some reactions from *Saccharomyces cerevisiae* model iMM904 (Mo et al., 2009) were incorporated in order to avoid missing reactions (Supplementary data Table S4).

Cell mass formation, given as Cell_mass_Eqn in Table S1, was also completed with Pi, H^+, H_2O and CoA. This modification provides a balanced ATP utilization in the cell mass reaction:

$$ATP + H_2O → ADP + Pi + H^+. \quad (8)$$

Then, the ATP hydrolyzed in this expression can be used for accounting the growth associated maintenance (GAM) (Feist et al., 2007). In addition, the protons consumed by the NAD(P)H associated reductions were also considered in the cell mass reaction.

Finally, a qualitative test of relevance was used to verify energetic (ATP) and redox consistency (NADH and NADPH). To this end, the exchange flux of the four carbon sources available in the model was set to zero and the reactions ATPM, NADPH_drain (Eq. (9)) and NADH_drain (Eq. (10)) were maximized one at a time. For the curated model, no feasible solution was found during the test of relevance meaning that there is no production of ATP and NAD(P)H in the absence of a carbon flux.

$$NADPH → NADP + H^+. \quad (9)$$

$$NADH → NAD + H^+. \quad (10)$$

The complete list of modified reactions with the corresponding references are given in the Supplementary data (Tables S3 and S4).

2.2.3. Compartmentalization of the model

As a result of the incorporation of new metabolites for mass balance, transport reactions for metabolites moving between compartments should be revised. The exchange reactions between extracellular space and cytosol, indicated with the prefix 'EX_' in Table S1, were included for the metabolites added during mass and charge balance. In the particular case of protons, a cytosolic ATPase was considered for their exchange with the extracellular medium (Liu et al., 2009). It is worth noting that the importance of ATPase reactions to maintain intracellular pH has been previously reported by Mondala et al. (2012). In addition, transporters between mitochondria and cytosol were also revised and updated accordingly. Diffusion through membranes was considered only for O_2, H_2O and CO_2. Finally, since ATP and ADP were not compartmentalized in the original model, an ADP-ATP translocator was incorporated to exchange the ATP generated by oxidative phosphorylation through the mitochondrial membrane (Liu et al., 2009). More details are provided in Supplementary data Sections S1.2.2 and S1.2.3.

2.3. In silico analysis of the metabolic network

In Bommareddy et al. (2015), the theoretical maximum yield of TAG and cell mass was calculated for each carbon source from the flux distribution obtained by Elementary Mode (EM) analysis. An EM represents a non-decomposable, stoichiometrically and thermodynamically feasible route for the conversion of substrates into products. In biological terms it can be used to determine the capability of a metabolic network, this is to estimate all the phenotypes that can be

Table 2
Theoretical maximum ATP yield for different carbon sources.

Carbon source	$y_{ATP/S}$ (mmol ATP/mmol S)
Glucose	16.8
Glycerol	9.75
Xylose	14
Arabinose	13.67

Substrate uptake: −1 mmol/(gDCW h).

expressed (Schuster et al., 2000; Papin et al., 2004) (also see references therein). From all the calculated EMs it is possible to obtain a set of EMs where the yield of a certain product is maximum for a defined carbon source, this is why it is used to calculate theoretical yields. However, EMs enumeration is computationally expensive due to the combinatorial explosion in the number of EMs as the network size increases (Machado and Herrgård, 2015), and only non-adjustable constraints are used to define it (Llaneras and Picó, 2008). Consequently, adjustable constraints that incorporate experimental measurements and regulation cannot be included in this methodology. In contrast, FBA is a predictive technique that assumes an optimal behavior of the microbial cell under certain adjustable and non-adjustable constraints, which can be modified to simulate different culture conditions. In addition, this approach is easy to scale towards large metabolic networks (Costa et al., 2016). FBA can be also used to calculate the maximum yield of the desired product from an optimal flux distribution obtained by setting an adequate reaction as the objective function.

For the general purpose of this work, there is no impediment to use any of the techniques described above. Nevertheless, we consider that FBA is more practical and has more potential for our future studies, in particular, to incorporate adjustable constraints.

To determine the flux distribution by FBA, the COBRA toolbox (Schellenberger et al., 2011) was used. The computational methods for model analysis and simulation are extensively described in Supplementary data Section S2.

The metabolism of *R. toruloides* was simulated under different environmental conditions to predict the maximum yields of cell mass and TAG using the curated metabolic model. Simulation within the FBA framework requires a linear objective function to be maximized (Supplementary data Section S2.1). Predictions of the optimal network state and the corresponding flux distribution are highly dependent on the objective function being used (Feist and Palsson, 2010).

In the curated model, the cell mass reaction represents the residual cell mass (i.e. only structural lipids are considered), whereas TAG is the net amount of lipids. By distinguishing these fractions the composition of cell mass is not altered by lipid accumulation. Otherwise, as was recently reported by Shen et al. (2017), the *R. toruloides* composition changes under nitrogen limitation at high consumed C/N ratios, where lipogenesis takes place. Taking this into account, the objective function was rationally chosen in order to predict the behavior of the cell under different conditions. First, in a culture condition where carbon is the limiting nutrient, the cell mass reaction (Cell_mass_Eqn in Table S1) was set as the objective function to replicate the main evolutionary purpose of the microorganism, which is survival. This objective function proved to be the most accurate when compared with experimental measurements (Llaneras and Picó, 2008). On the contrary, under nitrogen limitation and excess of carbon source, TAG production (TAGEx in Table S1) was chosen as the objective function. This is to simulate that in oleaginous microorganisms, under the limitation of a growth essential nutrient (such as nitrogen), the carbon source is partly derived to the synthesis of TAG (carbon overflow metabolism). This fact is independent of the culture mode (batch, fed-batch, and continuous culture). In the curated version of the model, FBA allows simulating the cell mass production in a nitrogen limiting culture by constraining the nitrogen uptake. As cell mass is the only product of the metabolism that consumes nitrogen, cell mass production is proportional to nitrogen uptake. Then, if this precursor is completely depleted, there is no flux of cell mass. Consequently, the carbon source is channeled to TAG production thus obtaining the theoretical maximum TAG yield.

Another constraint that is needed in order to apply FBA is the ATP requirement for non-growth associated maintenance (NGAM). The non-growth components included and determined empirically when measuring maintenance are (1) shifts in metabolic pathways, (2) energy spilling reactions, (3) cell motility, (4) changes in stored polymeric carbon, (5) osmoregulation, (6) extracellular losses of compounds not involved in osmoregulation, (7) proofreading, synthesis and turnover of macromolecular compounds such as enzymes and RNA, and (8) defense against O_2 stress (Van Bodegom, 2007). In the curated model there are two reactions that represent NGAM requirements: a cytosolic ATPase (ATPS) and the pseudoreaction ATPM. ATPS reaction is used to maintain physiological pH by excreting the excess of protons that are produced as a result of metabolism. On the other hand, ATPM is a reaction incorporated for modeling purposes, which considers all the reactions of the metabolism that consume ATP and were not included in the model. Since ATPM represents wasted energy for the cell, its flux is zero unless a minimum value is incorporated as a lower bound (Orth et al., 2010). The minimum flux of this reaction can be determined by means of the following equation:

$$v_{NGAM} = m_s \times y_{ATP/S} \quad (11)$$

where m_s is the maintenance coefficient and $y_{ATP/S}$ is the theoretical maximum yield of ATP for a defined substrate. The m_s coefficient for glucose was estimated from experimental data in Shen et al. (2013), whereas the $y_{ATP/S}$ was computed from the curated model by optimizing the ATPM objective reaction for a substrate uptake of −1 mmol/(gDCW h) (Orth et al., 2010) using FBA (Table 2).

3. Results and discussion

3.1. Small scale metabolic model for lipid production in R. toruloides

The small scale metabolic model for *R. toruloides* resulting from manual curation of the original model is illustrated in Fig. 2. It includes 93 metabolites: 82 internal and 11 external, and 104 reactions: 81 intracellular reactions, 10 transport reactions from cytosol to the extracellular medium, 11 exchange reactions with the environment (prefix 'EX') and 2 reactions of net production (GrowthEx and TAGEx).

As in the original reconstruction, this model includes the central carbon metabolism represented by glycolysis, PP pathway, TCA cycle and glyoxylate cycle and four carbon sources (glucose, glycerol, xylose, and arabinose). Glycerol is an attractive carbon source since it is a subproduct of biodiesel production (Koutinas et al., 2014). In addition, since xylose and arabinose are renewable and low-cost raw materials, they constitute an interesting alternative to conventional carbon sources (Papanikolaou and Aggelis, 2011b). The model is compartmentalized in the cytoplasmic and mitochondrial compartments which are connected by the corresponding transport reactions. Additionally, central nitrogen metabolism is represented by ammonium assimilation and the biosynthesis of glutamate and glutamine which are now cell mass precursors. Finally, the model also includes the pseudo-reaction that represents cell mass production from the metabolic precursors (Cell_mass_Eqn) and non-structural lipids synthesis represented by the TAG reaction (C51). These reactions were completed and balanced accordingly.

3.2. Analysis of the capability of cell metabolism using FBA

In order to determine the capabilities of cell metabolism, we studied the network as a whole and analyzed the pathways that take place under different culture conditions: carbon limitation and excess of nitrogen (case 1) and nitrogen exhaustion and excess of carbon (case 2),

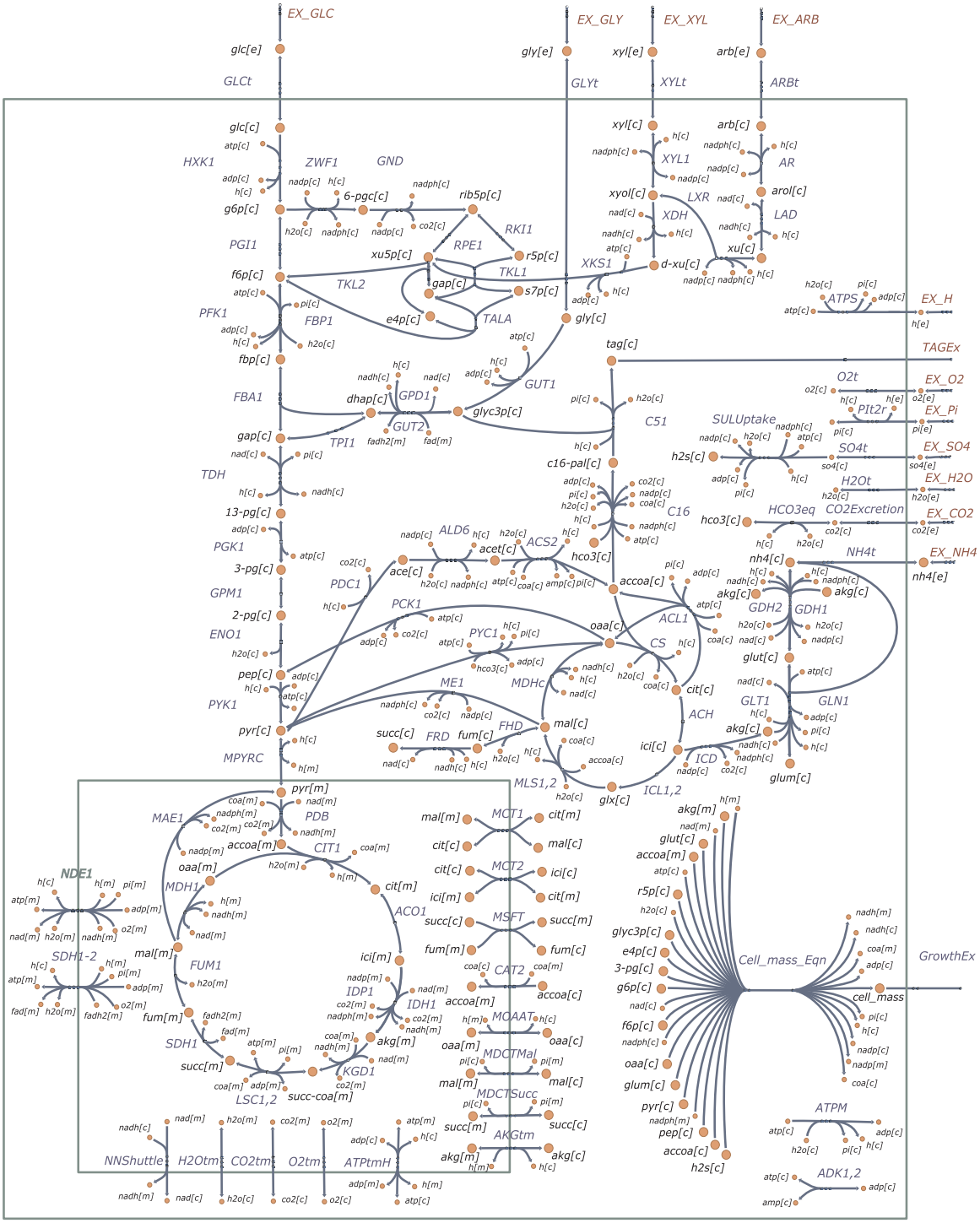

Fig. 2. Metabolic map of *R. toruloides*. The symbol ● represents primary metabolites while ● represents secondary metabolites. Cytosol and Mitochondria compartments are delimited by the dark green line. Metabolites h, pi, coa, and h2o were incorporated during model curation. Reactions 'EX_GLC', 'EX_GLY', 'EX_ARB' and 'EX_XYL' can be used to adjust carbon source uptake. To optimize cell mass formation and lipid production the FBA objective functions are 'Cell_mass_Eqn' and 'TAGEx', respectively. This map was generated with Escher (King et al., 2015). (For interpretation of the references to color in this figure legend, the reader is referred to the web version of the article.)

for all the carbon sources in the curated model.

With glucose as the sole carbon and energy source, a flux distribution for optimal growth (case 1) is shown in Fig. 3A. As expected, the fluxes through glycolysis and TCA cycle were high. These pathways, coupled to the respiratory chain, provide the ATP needed for cell mass synthesis. In addition, due to the incorporation of nitrogen precursors in the cell mass reaction, the central nitrogen metabolism was unblocked resulting in a net flux through ammonium transport reaction (NH4t) and the anabolic reactions GDH1 and GLN1. Notice that, under carbon limitation, there was no net flux in the reactions involved in TAG production (C16 and C51). These results were consistent with experimental observations in continuous cultures (Shen et al., 2013). Recall that structural lipids were considered in the cell mass fraction, which represents the 'residual cell mass' in this model.

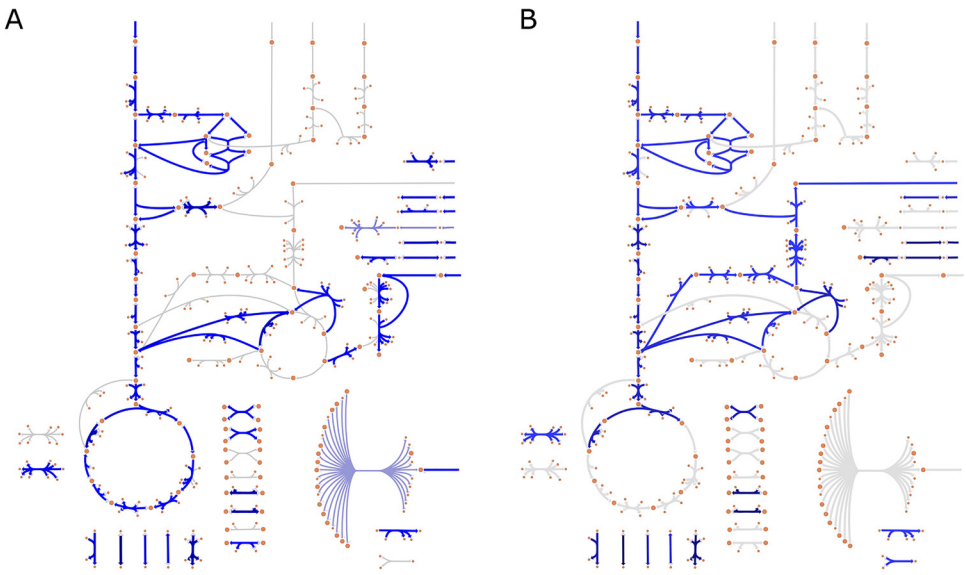

Fig. 3. A feasible flux distribution for optimal growth (A) and optimal TAG production (B) with glucose as carbon source. Reactions with blue arrows have nonzero fluxes. Refer to Fig. 2 for label details and Supplementary data (Table S5) to see the flux values of these distributions. (For interpretation of the references to color in this figure legend, the reader is referred to the web version of the article.)

On the other hand, when TAG reaction (C51) was the objective function (case 2), the flux distribution changed significantly (Fig. 3B). As it was mentioned before, the *de novo* lipogenesis in this model has two key steps: (i) biosynthesis of FAs and (ii) TAGs assembly from esterification of FAs with glyc3p. The stage (i) is induced in oleaginous yeasts under nitrogen limitation. The biochemical process starts with the decrease of intracellular AMP, which leads to the deactivation of NAD-dependent isocitrate dehydrogenase (IDH1). As a result, citrate is accumulated in the mitochondria at critical levels, so it must be transported to the cytosol via the mitochondrial malate transporter (MCT1). Cytoplasmatic citrate is then used to produce acetyl-CoA by ATP citrate lyase (ACL1), which is the main source of AcCoA for FAs synthesis in oleaginous yeast (Papanikolaou and Aggelis, 2011a; Zhu et al., 2012). The required AcCoA can also be provided by the acetyl-CoA synthetase (ACS2). It was found that ACS2 level increases during lipogenesis in *R. toruloides* (Zhu et al., 2012). In addition, in oleaginous microorganisms the reducing power (NADPH) needed for FAs biosynthesis is supplied by the NADP-malic enzyme (ME1) and glucose 6-phosphate dehydrogenase (ZWF1). In *R. toruloides*, ZWF1 is upregulated during lipogenesis (Zhu et al., 2012). Furthermore, ME1 protein level also increases during lipid production. ME1 is part of the transhydrogenation machinery together with pyruvate carboxylase (PYC1) and malate dehydrogenase (MDHc) (Zhu et al., 2012). As can be seen in Fig. 3B, under complete nitrogen exhaustion, glycolysis reactions were intensified and TCA reactions were impaired. This was in agreement with previous experimental observations of Zhu et al. (2012). There was also a high flux of MCT1 through cytosolic citrate. Besides, AcCoA was produced mainly by ACL1 with almost six times higher flux than ACS2 (Supplementary data Table S5). From the flux distribution map, NADPH was provided by PP pathway (ZWF1) and ME1, and there was a net flux in PYC1 and MDHc. In stage (ii) of lipid production, the FAs synthesized in stage (i) are esterified with glyc3p. When glucose was the carbon source, the required glyc3p was provided by glycerol-3-phosphate dehydrogenase (GPD), which was found at high levels during lipogenesis in *R. toruloides* (Zhu et al., 2012). In Fig. 3B, GDP was the only reaction that provided glyc3p with glucose as carbon source. Notice that the cell mass reaction had zero flux in the simulated scenario. This is a theoretical optimal state of TAG production that will be achieved under negligible amounts of nitrogen in the culture medium.

Through the analysis of the flux distributions obtained by FBA with glucose as sole carbon source under different culture conditions (case 1 and case 2) it was possible to replicate the metabolic changes that occur in *R. toruloides* during growth and lipogenesis, respectively. Similar results were obtained when glycerol, xylose, and arabinose were used as carbon source (Supplementary data, Section S3.1).

3.3. Effect of model curation in cell mass and TAG optimal yields

Once the optimal flux distributions for cell mass and TAG were obtained for all the available carbon and energy sources in the model, maximum yields were calculated as follows:

$$Y_{X/S} = \frac{v_X}{v_S} \tag{12}$$

$$Y_{\mathrm{TAG}/S} = \frac{v_L}{v_S} \tag{13}$$

where v_X is the growth flux in h^{-1}, v_S is the substrate flux in mmol/(gDCW h) and v_L is the TAG flux in mmol/(gDCW h). For residual cell mass, a molecular weight of 26.2 gDCW/Cmol was calculated from the elemental formula, considering a 3.5% of ashes (Shen et al., 2017). In addition, TAG was assumed as $C_{51}H_{98}O_6$ with a molecular weight 807.34 g/mol.

In Fig. 4, production envelopes for TAG and cell mass yields calculated using the original and the curated model are shown. Even when TAG maximum yield was not altered, the modifications incorporated during model curation resulted in a lower cell mass maximum yield for all carbon and energy sources. After analyzing the possible reasons for these differences, we found that the decrease in cell mass yields was the result of the incorporation of nitrogen precursors (glut and glum) in the cell mass reaction and the addition of protons during mass and charge balance. First, the reactions involved in glut and glum biosynthesis (GDH1 and GLN1) require reducing power (NADPH) and energy (ATP) with the concomitant reduction of their availability for cell mass biosynthesis. Since nitrogen is not involved in TAG production, the optimal yields were not affected by the unblocking of central nitrogen metabolism. On the other hand, the addition of protons in the model has a minor effect in reducing cell mass yield. The assimilation of all the carbon sources in the model generated internal protons that should be excreted to the environment (culture medium) in order to maintain physiological pH. Thereby, the energetic cost of pH regulation in the cell leads to a lower cell mass yield. For more details see Supplementary data, Section S3.2.

All these biochemical changes can be simulated only with the curated model since there are no protons and nitrogen precursors in the cell mass reaction of the original model.

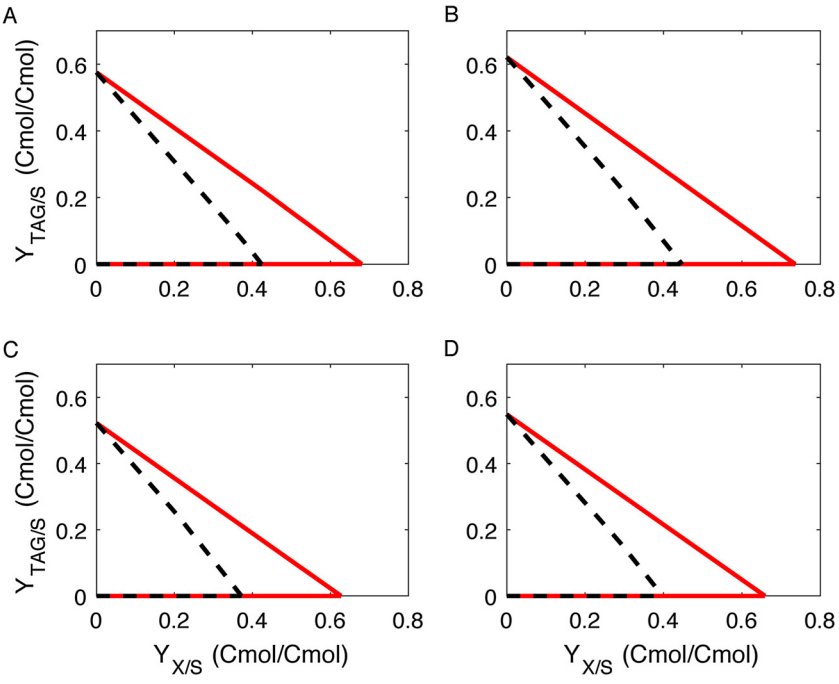

Fig. 4. Production envelopes for the sole carbon sources: (A) glucose, (B) glycerol, (C) arabinose and (D) xylose. In the curated model (dashed line), a lower growth is obtained in comparison with the original model (red line). The yields for TAG and cell mass were calculated with a maximum carbon uptake rate of −3 mmol/(gDCW h), without restriction of nitrogen uptake. (For interpretation of the references to color in this figure legend, the reader is referred to the web version of the article.)

4. Conclusion

In this work, we presented a curated version of a small-scale metabolic model for *de novo* lipid production by *R. toruloides*. During the curation process, the central nitrogen metabolism, essential to predict the lipid metabolism at different culture conditions, was unblocked. Moreover, the process of mass and charge balancing incorporated additional restrictions to cell mass production. Then, more rigorous theoretical maximum yields were obtained. The application of FBA for the network analysis resulted in some advantages. In particular, the possibility of including adjustable constraints allowed incorporating a minimum bound for ATPM with the concomitant reduction of the ATP available for growth and TAG production. In future studies, this model will be used to simulate the simultaneous cell mass and TAG production under different C/N ratios.

The contributions made in this work are the starting point for the generation of a genome-scale model to elucidate the complete metabolism of *R. toruloides*.

Acknowledgements

This work was supported by Universidad Nacional de La Plata (Project 11/I216), the National Research Council CONICET (PIP 112-201501-00837) and Agencia Nacional de Promoción Científica y Tecnológica (PICT 2014-2394) of Argentina.

Appendix A. Supplementary data

Supplementary data associated with this article can be found, in the online version, at https://doi.org/10.1016/j.jbiotec.2018.05.010.

References

Ageitos, J.M., Vallejo, J.A., Veiga-Crespo, P., Villa, T.G., 2011. Oily yeasts as oleaginous cell factories. Appl. Microbiol. Biotechnol. 90, 1219–1227.
Béligon, V., Christophe, G., Fontanille, P., Larroche, C., 2016. Microbial lipids as potential source to food supplements. Curr. Opin. Food Sci. 7, 35–42.
Bommareddy, R.R., Sabra, W., Maheshwari, G., Zeng, A.P., 2015. Metabolic network analysis and experimental study of lipid production in *Rhodosporidium toruloides* grown on single and mixed substrates. Microb. Cell Factories 14, 1–13.
Cherry, J.M., Hong, E.L., Amundsen, C., Balakrishnan, R., Binkley, G., Chan, E.T., Christie, K.R., Costanzo, M.C., Dwight, S.S., Engel, S.R., Fisk, D.G., Hirschman, J.E., Hitz, B.C., Karra, K., Krieger, C.J., Miyasato, S.R., Nash, R.S., Park, J., Skrzypek, M.S., Simison, M., Weng, S., Wong, E.D., 2012. *Saccharomyces* Genome Database: the genomics resource of budding yeast. Nucleic Acids Res. 40, D700–D705.
Costa, R.S., Hartmann, A., Vinga, S., 2016. Kinetic modeling of cell metabolism for microbial production. J. Biotechnol. 219, 126–141.
Edwards, J.S., Covert, M., Palsson, B., 2002. Metabolic modelling of microbes: the flux-balance approach. Environ. Microbiol. 4, 133–140.
Fei, Q., O'Brien, M., Nelson, R., Chen, X., Lowell, A., Dowe, N., 2016. Enhanced lipid production by *Rhodosporidium toruloides* using different fed-batch feeding strategies with lignocellulosic hydrolysate as the sole carbon source. Biotechnol. Biofuels 9, 130.
Feist, A.M., Henry, C.S., Reed, J.L., Krummenacker, M., Joyce, A.R., Karp, P.D., Broadbelt, L.J., Hatzimanikatis, V., Palsson, B.Ø., 2007. A genome-scale metabolic reconstruction for *Escherichia coli* K-12 MG1655 that accounts for 1260 ORFs and thermodynamic information. Mol. Syst. Biol. 3, 121.
Feist, A.M., Palsson, B.O., 2010. The biomass objective function. Curr. Opin. Microbiol. 13, 344–349.
Freitas, C., Parreira, T.M., Roseiro, J., Reis, A., da Silva, T.L., 2014. Selecting low-cost carbon sources for carotenoid and lipid production by the pink yeast *Rhodosporidium toruloides* NCYC 921 using flow cytometry. Bioresour. Technol. 158, 355–359.
Karamerou, E.E., Theodoropoulos, C., Webb, C., 2017. Evaluating feeding strategies for microbial oil production from glycerol by *Rhodotorula glutinis*. Eng. Life Sci. 17, 314–324.
Kauffman, K.J., Prakash, P., Edwards, J.S., 2003. Advances in flux balance analysis. Curr. Opin. Biotechnol. 14, 491–496.
Kavšček, M., Bhutada, G., Madl, T., Natter, K., 2015. Optimization of lipid production with a genome-scale model of *Yarrowia lipolytica*. BMC Syst. Biol. 9, 72.
King, Z.A., Dräger, A., Ebrahim, A., Sonnenschein, N., Lewis, N.E., Palsson, B.Ø., 2015. Escher: A Web Application for Building, Sharing, and Embedding Data-Rich Visualizations of Biological Pathways. PLOS Comput. Biol. 11, 1–13.
King, Z.A., Lu, J., Dräger, A., Miller, P., Federowicz, S., Lerman, J.A., Ebrahim, A., Palsson, B.Ø., Lewis, N.E., 2016. BiGG Models: a platform for integrating, standardizing and sharing genome-scale models. Nucleic Acids Res. 44, D515–D522.
Koutinas, A.A., Chatzifragkou, A., Kopsahelis, N., Papanikolaou, S., Kookos, I.K., 2014. Design and techno-economic evaluation of microbial oil production as a renewable resource for biodiesel and oleochemical production. Fuel 116, 566–577.
Kumar, S., Kushwaha, H., Bachhawat, A.K., Raghava, G.P.S., Ganesan, K., 2012. Genome Sequence of the Oleaginous Red Yeast *Rhodosporidium toruloides* MTCC 457. Eukaryot. Cell 11, 1083–1084.
Ling, J., Nip, S., Shim, H., 2013. Enhancement of lipid productivity of *Rhodosporidium toruloides* in distillery wastewater by increasing cell density. Bioresour. Technol. 146, 301–309.
Liu, H., Zhao, X., Wang, F., Li, Y., Jiang, X., Ye, M., Zhao, Z.K., Zou, H., 2009. Comparative proteomic analysis of *Rhodosporidium toruloides* during lipid accumulation. Yeast 26, 553–566.
Ljungdahl, P.O., Daignan-Fornier, B., 2012. Regulation of Amino Acid, Nucleotide, and Phosphate Metabolism in *Saccharomyces cerevisiae*. Genetics 190, 885–929.
Llaneras, F., Picó, J., 2008. Stoichiometric modelling of cell metabolism. J. Biosci. Bioeng. 105, 1–11.
Loira, N., Dulermo, T., Nicaud, J.M., Sherman, D.J., 2012. A genome-scale metabolic model of the lipid-accumulating yeast *Yarrowia lipolytica*. BMC Syst. Biol. 6, 35.
Machado, D., Herrgård, M.J., 2015. Co-evolution of strain design methods based on flux

balance and elementary mode analysis. Metab. Eng. Commun. 2, 85–92.
Magrane, M., UniProt Consortium, 2011. UniProt Knowledgebase: a hub of integrated protein data. Database J. Biol. Databases Curation 2011.
Mishra, P., Park, G.Y., Lakshmanan, M., Lee, H.S., Lee, H., Chang, M.W., Ching, C.B., Ahn, J., Lee, D.Y., 2016. Genome-scale metabolic modeling and in silico analysis of lipid accumulating yeast *Candida tropicalis* for dicarboxylic acid production. Biotechnol. Bioeng. 113, 1993–2004.
Mo, M.L., Palsson, B.Ø., Herrgård, M.J., 2009. Connecting extracellular metabolomic measurements to intracellular flux states in yeast. BMC Syst. Biol. 3, 37.
Mondala, A., Hernandez, R., French, T., McFarland, L., Sparks, D., Holmes, W., Haque, M., 2012. Effect of acetic acid on lipid accumulation by glucose-fed activated sludge cultures. J. Chem. Technol. Biotechnol. 87, 33–41.
Orij, R., Postmus, J., Ter Beek, A., Brul, S., Smits, G.J., 2009. *In vivo* measurement of cytosolic and mitochondrial pH using a pH-sensitive GFP derivative in *Saccharomyces cerevisiae* reveals a relation between intracellular pH and growth. Microbiology 155, 268–278.
Orth, J.D., Thiele, I., Palsson, B.Ø., 2010. What is flux balance analysis? Nat. Biotechnol. 28, 245–248.
Pan, P., Hua, Q., 2012. Reconstruction and *In Silico* Analysis of Metabolic Network for an OleaginousYeast, *Yarrowia lipolytica*. PLoS ONE 7, 1–11.
Papanikolaou, S., Aggelis, G., 2011a. Lipids of oleaginous yeasts. Part I: biochemistry of single cell oil production. Eur. J. Lipid Sci. Technol. 113, 1031–1051.
Papanikolaou, S., Aggelis, G., 2011b. Lipids of oleaginous yeasts. Part II: technology and potential applications. Eur. J. Lipid Sci. Technol. 113, 1052–1073.
Papin, J.A., Stelling, J., Price, N.D., Klamt, S., Schuster, S., Palsson, B.O., 2004. Comparison of network-based pathway analysis methods. Trends Biotechnol. 22, 400–405.
Rutter, C.D., Zhang, S., Rao, C.V., 2015. Engineering *Yarrowia lipolytica* for production of medium-chain fatty acids. Appl. Microbiol. Biotechnol. 99, 7359–7368.
Schellenberger, J., Que, R., Fleming, R.M.T., Thiele, I., Orth, J.D., Feist, A.M., Zielinski, D.C., Bordbar, A., Lewis, N.E., Rahmanian, S., Kang, J., Hyduke, D.R., Palsson, B.Ø., 2011. Quantitative prediction of cellular metabolism with constraint-based models: the COBRA Toolbox v2.0. Nat. Protoc. 6, 1290–1307.
Schuster, S., Fell, D.A., Dandekar, T., 2000. A general definition of metabolic pathways useful for systematic organization and analysis of complex metabolic networks. Nat. Biotechnol. 18, 326–332.
Shen, H., Gong, Z., Yang, X., Jin, G., Bai, F., Zhao, Z.K., 2013. Kinetics of continuous cultivation of the oleaginous yeast *Rhodosporidium toruloides*. J. Biotechnol. 168, 85–89.
Shen, H., Zhang, X., Gong, Z., Wang, Y., Yu, X., Yang, X., Zhao, Z.K., 2017. Compositional profiles of *Rhodosporidium toruloides* cells under nutrient limitation. Appl. Microbiol. Biotechnol. 101, 3801–3809.
Van Bodegom, P., 2007. Microbial Maintenance: A Critical Review on Its QuantificationMicrobial Ecology. Microb. Ecol. 53, 513–523.
Varma, A., Palsson, B.O., 1994. Metabolic flux balancing: basic concepts, scientific and practical use. Nat. Biotechnol. 12, 994–998.
Wu, S., Hu, C., Jin, G., Zhao, X., Zhao, Z.K., 2010. Phosphate-limitation mediated lipid production by *Rhodosporidium toruloides*. Bioresour. Technol. 101, 6124–6129.
Wu, S., Zhao, X., Shen, H., Wang, Q., Zhao, Z.K., 2011. Microbial lipid production by *Rhodosporidium toruloides* under sulfate-limited conditions. Bioresour. Technol. 102, 1803–1807.
Xu, J., Du, W., Zhao, X., Zhang, G., Liu, D., 2013. Microbial oil production from various carbon sources and its use for biodiesel preparation. Biofuels Bioprod. Biorefin. 7, 65–77.
Xu, J., Zhao, X., Wang, W., Du, W., Liu, D., 2012. Microbial conversion of biodiesel by-product glycerol to triacylglycerols by oleaginous yeast *Rhodosporidium toruloides* and the individual effect of some impurities on lipid production. Biochem. Eng. J. 65, 30–36.
Xue, Z., Sharpe, P.L., Hong, S.P., Yadav, N.S., Xie, D., Short, D.R., Damude, H.G., Rupert, R.A., Seip, J.E., Wang, J., Pollak, D.W., Bostick, M.W., Bosak, M.D., Macool, D.J., Hollerbach, D.H., Zhang, H., Arcilla, D.M., Bledsoe, S.A., Croker, K., McCord, E.F., Tyreus, B.D., Jackson, E.N., Zhu, Q., 2013. Production of omega-3 eicosapentaenoic acid by metabolic engineering of *Yarrowia lipolytica*. Nat. Biotechnol. 31, 734–740.
Yang, X., Jin, G., Gong, Z., Shen, H., Bai, F., Zhao, Z.K., 2014. Recycling biodiesel-derived glycerol by the oleaginous yeast *Rhodosporidium toruloides* Y4 through the two-stage lipid production process. Biochem. Eng. J. 91, 86–91.
Yang, X., Jin, G., Wang, Y., Shen, H., Zhao, Z.K., 2015. Lipid production on free fatty acids by oleaginous yeasts under non-growth conditions. Bioresour. Technol. 193, 557–562.
Ye, C., Xu, N., Chen, H., Chen, Y.Q., Chen, W., Liu, L., 2015. Reconstruction and analysis of a genome-scale metabolic model of the oleaginous fungus *Mortierella alpina*. BMC Syst. Biol. 9, 1.
Zhang, H., Zhang, L., Chen, H., Chen, Y.Q., Chen, W., Song, Y., Ratledge, C., 2014. Enhanced lipid accumulation in the yeast *Yarrowia lipolytica* by over-expression of ATP: citrate lyase from *Mus musculus*. J. Biotechnol. 192, 78–84.
Zhao, X., Hu, C., Wu, S., Shen, H., Zhao, Z.K., 2011. Lipid production by *Rhodosporidium toruloides* Y4 using different substrate feeding strategies. J. Ind. Microbiol. Biotechnol. 38, 627–632.
Zhao, X., Wu, S., Hu, C., Wang, Q., Hua, Y., Zhao, Z.K., 2010. Lipid production from Jerusalem artichoke by *Rhodosporidium toruloides* Y4. J. Ind. Microbiol. Biotechnol. 37, 581–585.
Zhou, W., Li, Y., Zhang, Y., Zhao, Z., 2012. Energy efficiency evaluation of lipid production by oleaginous yeast *Rhodosporidium toruloides*. J. Therm. Anal. Calorim. 108, 119–126.
Zhu, Z., Zhang, S., Liu, H., Shen, H., Lin, X., Yang, F., Zhou, Y.J., Jin, G., Ye, M., Zou, H., Zhao, Z.K., 2012. A multi-omic map of the lipid-producing yeast *Rhodosporidium toruloides*. Nat. Commun. 3, 1112.